



| | |
|------------------|---|
| Title | Pulse compression of phase-matched high harmonic pulses from a time-delay compensated monochromator |
| Author(s) | Igarashi, Hironori; Makida, Ayumu; Ito, Motohiko; Sekikawa, Taro |
| Citation | Optics Express, 20(4), 3725-3732 https://doi.org/10.1364/OE.20.003725 |
| Issue Date | 2012-02-13 |
| Doc URL | http://hdl.handle.net/2115/49089 |
| Rights | ©2012 Optical Society of America |
| Type | article |
| File Information | OE20-4_3725-3732.pdf |



[Instructions for use](#)

Pulse compression of phase-matched high harmonic pulses from a time-delay compensated monochromator

Hironori Igarashi, Ayumu Makida, Motohiko Ito, and Taro Sekikawa*

Department of Applied Physics, Hokkaido University, Kita 13 Nishi 8, Kita-ku, Sapporo 060-8628, Japan
[*sekikawa@eng.hokudai.ac.jp](mailto:sekikawa@eng.hokudai.ac.jp)

Abstract: Single 32.6 eV high harmonic pulses from a time-delay compensated monochromator were compressed down to 11 ± 3 fs by completely compensating for the pulse-front tilt. The photon flux was intensified up to 5.7×10^9 photons/s on target by implementing high harmonic generation under a phase matching condition in a hollow fiber used for increasing the interaction length. The output photon flux on target from the monochromator was comparable to that from a small synchrotron facility, while the pulse duration was more than three orders of magnitude shorter. This high harmonic beam line fulfills two requirements for time-resolved spectroscopy in extreme ultraviolet region, namely, ultrashort pulses and high photon flux.

©2012 Optical Society of America

OCIS codes: (190.4160) Multiharmonic generation; (320.5520) Pulse compression; (320.7100) Ultrafast measurements.

References and links

1. R. Haight and D. R. Peale, "Tunable photoemission with harmonics of subpicosecond lasers," *Rev. Sci. Instrum.* **65**(6), 1853–1857 (1994).
2. L. Nugent-Glandorf, M. Scheer, D. A. Samuels, V. M. Bierbaum, and S. R. Leone, "A laser-based instrument for the study of ultrafast chemical dynamics by soft x-ray-probe photoelectron spectroscopy," *Rev. Sci. Instrum.* **73**(4), 1875–1886 (2002).
3. P. Wernet, M. Odelius, K. Godehusen, J. Gaudin, O. Schwarzkopf, and W. Eberhardt, "Real-time evolution of the valence electronic structure in a dissociating molecule," *Phys. Rev. Lett.* **103**(1), 013001 (2009).
4. L. Poletto, P. Villoresi, F. Frassetto, F. Calegari, F. Ferrari, M. Lucchini, G. Sansone, and M. Nisoli, "Time-delay compensated monochromator for the spectral selection of extreme-ultraviolet high-order laser harmonics," *Rev. Sci. Instrum.* **80**(12), 123109 (2009).
5. M. Ito, Y. Kataoka, T. Okamoto, M. Yamashita, and T. Sekikawa, "Spatiotemporal characterization of single-order high harmonic pulses from time-compensated toroidal-grating monochromator," *Opt. Express* **18**(6), 6071–6078 (2010), <http://www.opticsinfobase.org/oe/abstract.cfm?URI=oe-18-6-6071>.
6. G. L. Dakovski, Y. Li, T. Durakiewicz, and G. Rodriguez, "Tunable ultrafast extreme ultraviolet source for time- and angle-resolved photoemission spectroscopy," *Rev. Sci. Instrum.* **81**(7), 073108 (2010).
7. F. Krausz and M. Ivanov, "Attosecond physics," *Rev. Mod. Phys.* **81**(1), 163–234 (2009).
8. L. Nugent-Glandorf, M. Scheer, D. A. Samuels, A. M. Mulhisen, E. R. Grant, X. Yang, V. M. Bierbaum, and S. R. Leone, "Ultrafast time-resolved soft x-ray photoelectron spectroscopy of dissociating Br₂," *Phys. Rev. Lett.* **87**(19), 193002 (2001).
9. T. Sekikawa, T. Yamazaki, Y. Nabekawa, and S. Watanabe, "Femtosecond Lattice Relaxation Induced by Inner-Shell Excitation," *J. Opt. Soc. Am. B* **19**(8), 1941–1945 (2002).
10. T. Shimizu, T. Sekikawa, T. Kanai, S. Watanabe, and M. Itoh, "Time-resolved Auger decay in CsBr using high harmonics," *Phys. Rev. Lett.* **91**(1), 017401 (2003).
11. T. Sekikawa, A. Kosuge, T. Kanai, and S. Watanabe, "Nonlinear optics in the extreme ultraviolet," *Nature* **432**(7017), 605–608 (2004).
12. M. Uiberacker, T. Uphues, M. Schultze, A. J. Verhoeve, V. Yakovlev, M. F. Kling, J. Rauschenberger, N. M. Kabachnik, H. Schröder, M. Lezius, K. L. Kompa, H.-G. Muller, M. J. J. Vrakking, S. Hendel, U. Kleineberg, U. Heinzmann, M. Drescher, and F. Krausz, "Attosecond real-time observation of electron tunnelling in atoms," *Nature* **446**(7136), 627–632 (2007).
13. T. Sekikawa, T. Okamoto, E. Haraguchi, M. Yamashita, and T. Nakajima, "Two-photon resonant excitation of a doubly excited state in He atoms by high-harmonic pulses," *Opt. Express* **16**(26), 21922–21929 (2008), <http://www.opticsinfobase.org/oe/abstract.cfm?URI=oe-16-26-21922>.

14. W. Li, X. Zhou, R. Lock, S. Patchkovskii, A. Stolow, H. C. Kapteyn, and M. M. Murnane, "Time-resolved dynamics in N_2O_4 probed using high harmonic generation," *Science* **322**(5905), 1207–1211 (2008).
15. Y. Nabekawa, T. Shimizu, Y. Furukawa, E. J. Takahashi, and K. Midorikawa, "Interferometry of attosecond pulse trains in the extreme ultraviolet wavelength region," *Phys. Rev. Lett.* **102**(21), 213904 (2009).
16. H. Wang, M. Chini, S. Chen, C.-H. Zhang, F. He, Y. Cheng, Y. Wu, U. Thumm, and Z. Chang, "Attosecond time-resolved autoionization of argon," *Phys. Rev. Lett.* **105**(14), 143002 (2010).
17. P. Villoresi, "Compensation of optical path lengths in extreme-ultraviolet and soft-x-ray monochromators for ultrafast pulses," *Appl. Opt.* **38**(28), 6040–6049 (1999).
18. F. Frassetto, P. Villoresi, and L. Poletto, "Optical concept of a compressor for XUV pulses in the attosecond domain," *Opt. Express* **16**(9), 6652–6667 (2008), <http://www.opticsinfobase.org/oe/abstract.cfm?URI=oe-16-9-6652>.
19. L. Poletto, P. Villoresi, E. Benedetti, F. Ferrari, S. Stagira, G. Sansone, and M. Nisoli, "Intense femtosecond extreme ultraviolet pulses by using a time-delay-compensated monochromator," *Opt. Lett.* **32**(19), 2897–2899 (2007).
20. L. Poletto, P. Villoresi, E. Benedetti, F. Ferrari, S. Stagira, G. Sansone, and M. Nisoli, "Intense femtosecond extreme ultraviolet pulses by using a time-delay-compensated monochromator: erratum," *Opt. Lett.* **33**(2), 140–140 (2008).
21. F. Frassetto, C. Cacho, C. A. Froud, I. C. E. Turcu, P. Villoresi, W. A. Bryan, E. Springate, and L. Poletto, "Single-grating monochromator for extreme-ultraviolet ultrashort pulses," *Opt. Express* **19**(20), 19169–19181 (2011), <http://www.opticsinfobase.org/oe/abstract.cfm?URI=oe-19-20-19169>.
22. L. Poletto and F. Frassetto, "Time-preserving grating monochromators for ultrafast extreme-ultraviolet pulses," *Appl. Opt.* **49**(28), 5465–5473 (2010).
23. P. Wernet, "Electronic structure in real time: mapping valence electron rearrangements during chemical reactions," *Phys. Chem. Chem. Phys.* **13**(38), 16941–16954 (2011).
24. A. Rundquist, C. G. Durfee 3rd, Z. Chang, C. Herne, S. Backus, M. M. Murnane, and H. C. Kapteyn, "Phase-matched generation of coherent soft X-rays," *Science* **280**(5368), 1412–1415 (1998).
25. Y. Tamaki, Y. Nagata, M. Obara, and K. Midorikawa, "Phase-matched high-order-harmonic generation in a gas-filled hollow fiber," *Phys. Rev. Lett.* **59**, 4041 (1999).
26. T. E. Glover, R. W. Schoenlein, A. H. Chin, and C. V. Shank, "Observation of laser assisted photoelectric effect and femtosecond high order harmonic radiation," *Phys. Rev. Lett.* **76**(14), 2468–2471 (1996).
27. L. Poletto, "Tolerances of time-delay-compensated monochromators for extreme-ultraviolet ultrashort pulses," *Appl. Opt.* **48**(23), 4526–4535 (2009).
28. M. Lewenstein, P. Balcou, M. Y. Ivanov, A. L'Huillier, and P. B. Corkum, "Theory of high-harmonic generation by low-frequency laser fields," *Phys. Rev. A* **49**(3), 2117–2132 (1994).
29. E. Constant, D. Garzella, P. Breger, E. Mével, C. Dorrer, C. Le Blanc, F. Salin, and P. Agostini, "Optimizing high harmonic generation in absorbing gases: model and experiment," *Phys. Rev. Lett.* **82**(8), 1668–1671 (1999).

1. Introduction.

High harmonics, which are generated under nonlinear interaction between atoms and ultrashort laser pulses, can be compact table-top ultrashort light sources in the extreme ultraviolet (XUV) and soft x-ray regions [1–6]. Since the pulse durations of high harmonics are in the femtosecond or attosecond regimes, high harmonics provide us with unique opportunities to investigate nonlinear optics and time-resolved spectroscopy in the XUV and soft x-ray regions, which researchers have not yet been able to study using synchrotron radiation [7–16].

However, applying high harmonics to spectroscopy is not straightforward because multiple orders of high harmonics are generated collinearly with intense driving laser pulses. It is necessary to choose an appropriate harmonic order for the application, especially for spectroscopy used to gain insight into electronic structures of materials. Although multilayer mirrors are useful optical elements for selecting one harmonic order, the contrast ratio of reflectivity is sometimes poor. The loose selection of one harmonic by multilayer mirrors sometimes leads to the creation of noise by the other harmonic orders, and this covers up the signals [13]. A monochromator employing a grating is a standard optical element for this purpose and was used in the pioneering work in this field [1]. However, it introduces a stretch of the pulse duration by the pulse-front tilt, compromising the advantages of high harmonics.

To select a single harmonic with the pulse duration preserved, a time-delay compensated monochromator (TDCM) consisting of a pair of gratings to compensate for the pulse-front tilt was proposed, and this approach has been experimentally and theoretically investigated [2, 5, 17–20]. The schematic of the TDCM that we developed, which consists of two toroidal gratings, is shown in Fig. 1 [5]. In our TDCM, multiple orders of high harmonic pulses were diffracted by the first grating and were focused on the slit, which was placed on the Fourier

plane of the first grating and which selected the harmonic order. The second grating compensated for the pulse-front tilt of the diffracted harmonic pulses.

One drawback of the TDCM is low throughput resulting from the diffraction efficiency of the grating. To overcome this weakness, a conical mount for the gratings was implemented to increase the diffraction efficiency. Although the throughput was improved to the range of 0.10–0.18, the optical configuration using six optical elements is relatively complicated [19, 20]. To simplify the configuration and to improve the throughput, a single grating configuration employing a grating with a lower dispersion for minimizing the pulse stretch was proposed and experimentally demonstrated: the system provided 1.6×10^7 photons/pulse at 32.5 eV with a pulse duration in the range of 20 to 30 fs [21, 22], in spite of compressibility down to 8 fs. In another system, a single grating configuration was employed for time-resolved photoelectron spectroscopy, though the time resolution was limited to 135 fs [23]. Thus, a compromise between the temporal resolution and the throughput of the monochromator has so far been necessary.

In this study, we attempted to balance these two competing requirements—short pulse duration and high photon flux—by compressing high harmonic pulses and by increasing the conversion efficiency of high harmonic generation. Although the pulse duration was compressed to 47 fs in the previous work [5], there still remains a question as to what limits the compressed pulse duration. We are particularly interested in the accuracy required for constructing the monochromator. In this work, we demonstrate pulse compression of the 21st harmonic pulses ($= 32.6$ eV) down to 11 ± 3 fs by adjusting the slit position located between the gratings. To improve the conversion efficiency, high harmonics were generated in a hollow fiber filled with rare gas to increase the interaction length under a phase-matched condition, which was found by changing the gas pressure inside the fiber [24, 25]. The final maximum photon flux was 5.7×10^6 photons/pulse on target, and that of the 19th harmonic was intensified to 7.1×10^6 photons/pulse.

2. Experimental setup

In this work, both to make the pulse duration shorter and to increase the power of the high harmonics, we altered the TDCM shown in Fig. 1 in the following two ways: i) A pulse gas jet was replaced with a gas-filled hollow fiber for high harmonic generation to enhance the conversion efficiency by satisfying the phase matching condition. ii) The slit was changed to be movable in the Fourier plane of the first grating for pulse compression.

The following laser system was used for high harmonic generation. 700 μ J Ti:sapphire laser pulses with a pulse duration of 26 fs at a repetition rate of 1 kHz were focused into a 1 cm-long, 300 μ m-diameter hollow fiber filled with static krypton gas by a concave mirror with a 50 cm radius. The peak intensity of the laser pulse inside the fiber was 4.7×10^{13} W/cm². The position of the fiber was adjusted along the direction of the beam propagation so that the output power was maximized. The photon flux of the separated high harmonic was measured using a calibrated XUV photodiode (AXUV-100, IRD Inc.). We also tried 2 cm- and 3 cm-long fibers, but the maximum photon flux was obtained using the 1 cm fiber.

The temporal duration of the selected high harmonic pulses was measured by observing the temporal evolution of the sideband peaks in the photoelectron spectra of Ne that were caused by the two-photon free-to-free transition under simultaneous irradiation of both XUV and fundamental photons [26]. The peak intensity of the probe was 1.3×10^{11} W/cm². The photoelectrons were energy analyzed by a magnetic bottle photoelectron spectrometer.

The characteristics of the toroidal grating (HORIBA Jobin Yvon, 54000910) used in the TDCM are as follows: The radii of curvature were 1 m and 104.09 mm in the horizontal and vertical directions, respectively. The focal lengths from the entrance and the exit were 319.9 and 319.5 mm, respectively. The groove density was 550 lines/mm with a variable pitch. The spectral dispersions were 2.07 nm/mm at 48.75 nm and 2.22 nm/mm at 82.5 nm. The maximum diffraction efficiency was 16% around 35 eV.

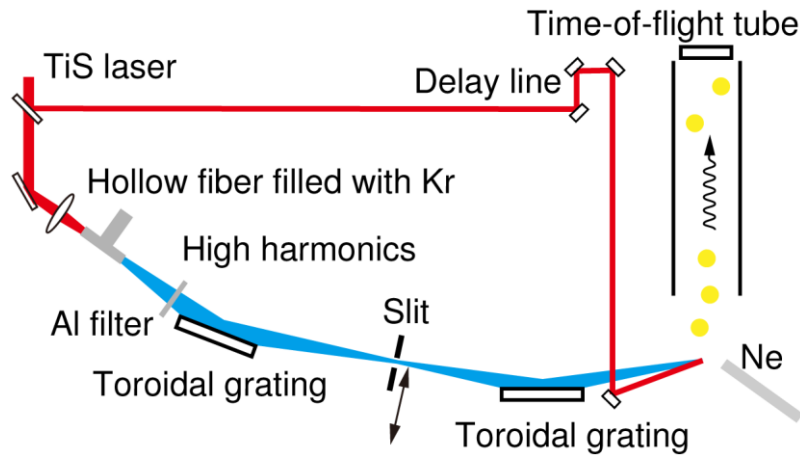


Fig. 1. Schematic of the time-delay compensated monochromator with toroidal gratings, including the experimental setup for high harmonic generation and temporal characterization by cross-correlation. The slit position was moved in the Fourier plane for pulse compression.

3. Pulse compression of selected harmonic pulses

The difference in the optical path lengths of two diffracted beams from the adjacent grooves on a grating is one wavelength λ in the case of the first order diffraction, and the total difference in the optical path length across the beam amounts to $N\lambda$, where N is the total number of illuminated grooves. Thus, although the wave front of the beam is still preserved after diffraction, the pulse front is tilted and the effective pulse duration is stretched by $N\lambda/c$. The basic idea of the TDCM is to compensate for this optical path difference $N\lambda$ by placing the second grating at the symmetrical position with respect to the slit [17]. For complete compensation, the illuminated areas of both gratings should be equal.

In a previous work, we found that the pulse duration was not compressed completely [5]. In our system, the emitting point of the high harmonics and the focus were fixed. Thus, when the incident angle to the second grating deviated from the planned angle, the diffraction angle of the second grating became different from that of the first grating. This led to different illuminated areas on the gratings, resulting in incomplete compression of the high harmonic pulses. Here, the incident angle to the second grating can be adjusted by displacing the slit position in the Fourier plane of the gratings.

Thus, firstly, the pulse stretch of the 21st harmonic in our TDCM system was estimated by a numerical simulation using the given parameters of the toroidal grating. Figure 2 shows the calculated pulse stretch arising from unequal irradiation areas on the gratings as a function of the slit position. At the origin, the irradiated areas of the two gratings become equal, and the pulse stretch is about 100 fs with 5 mm displacement of the slit. Therefore, it might be possible to compress the pulse duration by shifting the slit position by several millimeters. A similar pulse stretch resulting from the misalignment of the gratings in the TDCM was also numerically predicted using six optical components [27]. The estimated pulse stretch in Ref 27. was about five times smaller than in the present case. This is because the groove densities of the assumed grating were about five times lower than that of the toroidal gratings used in this TDCM.

The displacement of the slit by several millimeters was found to lengthen the pulse duration of the separated harmonic pulses. In other words, pulse compression can be achieved by moving the slit position along the Fourier plane of the grating. We measured the pulse duration of the 21st harmonic as a function of the slit position for pulse compression. Figure 3a and 3b show the cross-correlation between the 21st harmonic and the fundamental pulses at slit positions of 0 and 3 mm, respectively. Here, the origin of the slit position was defined as the slit position immediately after the initial experimental setup. The pulse duration of a

selected harmonic pulse was obtained by deconvoluting a high harmonic pulse from the cross-correlation by assuming harmonic and fundamental pulses to be Gaussian functions. Figure 3c shows that the pulse duration was compressed down to 11 ± 3 fs at a slit position of 3 mm from the initial position. Further shifts increased the pulse duration. The solid line in Fig. 3c is the calculated pulse stretch shifted by 11 fs and by 3 mm in the vertical and horizontal directions, respectively. The experimentally measured pulse duration was explained very well without reference to free parameters. Therefore, the deviation of the incident angle to the second grating from the optimum is the most crucial parameter in constructing the TDCM. To reduce the broadening to within $\pm 10\%$ of the optimum, the slit position should be determined to an accuracy of 0.1 mm.

The shortest compressed pulse duration of the 21st harmonic was 11 ± 3 fs. To determine the consistency, we calculated the pulse profile of the 21st harmonic from the single atom response under the strong-field approximation [28]. When the pulse duration of the driving laser was 30 fs, the pulse duration of the output harmonic pulse was 15 fs; this was almost consistent with the experimental results.

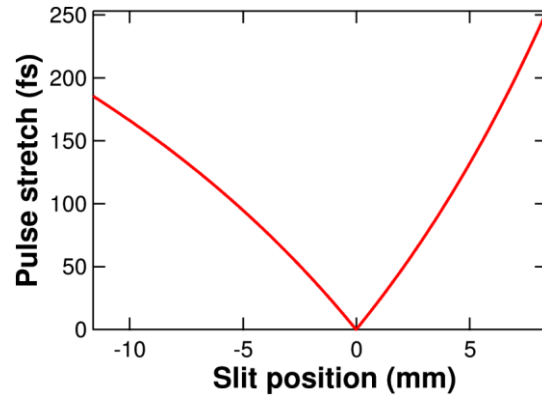


Fig. 2. Pulse stretch as a function of the slit position, determining the incident angle to the second grating.

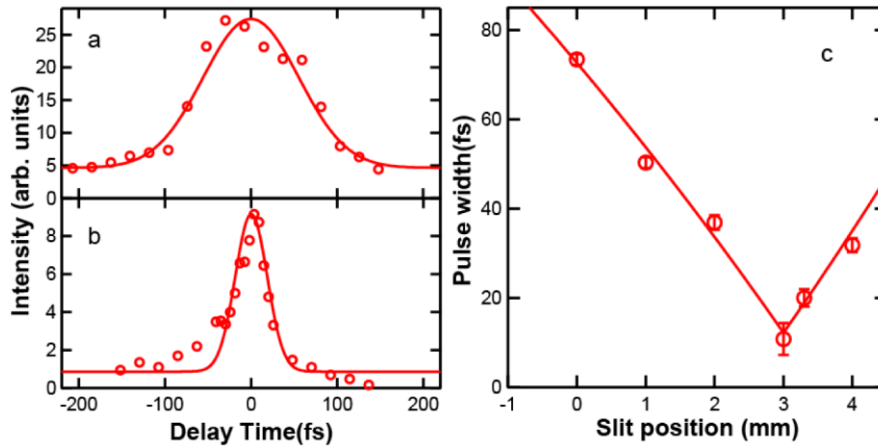


Fig. 3. Cross-correlation between the 21st harmonic and fundamental pulses at slit positions of (a) 0 mm and (b) 3 mm. The solid lines are the results of fitting to Gaussian functions. (c) Pulse duration of the 21st harmonic pulse as a function of slit position. The solid line is the numerically calculated pulse stretch shifted by the measured shortest pulse duration.

4. Enhancement of photon flux by phase matching

One drawback of the present TDCM is related to its total throughput of high harmonic pulses. Since the maximum diffraction efficiency of the toroidal grating we used was about 16%, the total throughput was only a few percent. Since higher photon flux is preferred for spectroscopic applications, we employed a phase matching technique to improve the conversion efficiency of high harmonic generation [24, 25].

The phase mismatch between the fundamental laser and high harmonics Δk is

$$\Delta k = \Delta k_{atom} + \Delta k_{ion} + \Delta k_{NL} + \Delta k_{fiber}, \quad (1)$$

where Δk_{atom} , Δk_{ion} , Δk_{NL} , and Δk_{fiber} are the dispersions of neutral atoms, of electrons, and of the nonlinear refraction index and the dispersion resulting from the structure of the hollow fiber, respectively [24]. Here, each component is expressed as follows:

$$\Delta k_{atom} + \Delta k_{NL} = -qp(1-\eta)\frac{2\pi}{\lambda_0}(\Delta\delta + n_2), \quad (2)$$

$$\Delta k_{ion} = qp\eta N_a r_e \lambda_0, \quad (3)$$

and

$$\Delta k_{fiber} = q\frac{u_{11}^2 \lambda_0}{4\pi a^2}, \quad (4)$$

where q denotes the harmonic order, p is the pressure, η is the ionization level, λ_0 is the wavelength of the fundamental laser, $\Delta\delta$ is the difference between the indices of refraction of the gas per atmosphere at the fundamental and harmonic fields, n_2 is the nonlinear index of refraction per atmosphere at λ_0 , N_a is the number density of atoms per atm, r_e is the classical electron radius, u_{11} is the mode factor of the hollow fiber, and a is the inner radius of the hollow fiber. Phase matching can be achieved by varying the gas pressure inside the hollow fiber. The cancelation of the negative dispersion by the positive dispersion resulting from free electrons is very important. Then, taking into account the absorption coefficient of the gas medium α , the phase mismatch factor $J(\Delta k)$ becomes

$$J(\Delta k) = \frac{1 + \exp(-\alpha L) - 2\cos(\Delta k L)\exp(-\alpha L/2)}{(\alpha/2)^2 + (\Delta k)^2}, \quad (5)$$

where L is the interaction length for high harmonic generation [29].

To find the conditions that maximize the conversion efficiency, we evaluated $(1 - N_{ion})^2 J(\Delta k)$ of a continuous 21st harmonic wave as a function of gas pressure at various degrees of ionization of gas medium N_{ion} (see Fig. 4). In this work, we used krypton gas because of its high nonlinearity compared with argon gas, and we set the fiber length to $L = 1$ cm. We accounted for $(1 - N_{ion})^2$ because of the lower nonlinear susceptibility of ionized atoms for high harmonics generation. The phase mismatch $\Delta k_{atom} + \Delta k_{NL}$ resulting from the dispersion of neutral atoms is cancelled out by the phase mismatch of ionized free electrons Δk_{ion} . Figure 4 shows that the conversion efficiency is governed by the phase mismatch at lower ionization degree less than 6%. On the other hand, at 7%, $(1 - N_{ion})^2 J(\Delta k)$ increases with gas pressure and the absorption by gas media limits the conversion efficiency [29]. This is due to the constructive contribution of negative $\cos(\Delta k L)$ in Eq. (5), which is realized by the cancellation of the phase mismatch due to ionization. Therefore, under a moderately ionized condition, it is possible to increase the gas pressure with a phase-matched condition satisfied, leading to the generation of more intense high harmonics, while the optimum gas pressure is limited by the phase mismatch under lower N_{ion} . Although Fig. 4 is for continuous wave, the preferable condition for high harmonic generation should be realized transiently with

temporal evolution of ultrashort pulses. Hence, qualitatively similar pressure dependence of the harmonic intensity is expected.

To experimentally find an optimum condition that increases the output power, the pressure dependence of the intensity of the 21st harmonic generated from Kr gas was measured; it is depicted in Fig. 5. When the length of the hollow fiber was 2 cm, the output intensity was found to have a maximum around 18 Torr, as shown in Fig. 5a. On the other hand, when the interaction length was 1 cm, the photon number increased with pressure and reached intensity saturation at over 90 Torr, as shown in Fig. 5b. The maximum output of 5.7×10^9 photons/s on target was obtained when the 1 cm hollow fiber was filled with 120 Torr krypton gas. Furthermore, a photon flux of 7.1×10^9 photons/s was obtained at the 19th harmonic ($= 29.6$ eV).

From the numerical simulation shown in Fig. 4, the pressure dependence of the harmonic intensity was found to change dramatically with N_{ion} : when N_{ion} is lower than 6%, the pressure dependence has a peak around 20 Torr. On the other hand, the phase mismatch factor has wider tolerance for pressure at $N_{\text{ion}} = 7\%$. These pressure dependencies agree well with the experimental results shown in Fig. 5: N_{ion} was assumed to be 6% and 7% in the solid lines in Fig. 5a and 5b, respectively. Although we tried to maintain the same focusing condition, N_{ion} appeared to be smaller in the 2 cm hollow fiber. This slight difference in N_{ion} might be attributable to the coupling loss from the laser beam to the hollow fiber and also to the propagation loss inside the hollow fiber. In order to increase the conversion efficiency, a longer interaction length is desired. However, we could not experimentally achieve better beam coupling to the 2 cm and 3 cm hollow fibers. Thus, we chose the 1 cm hollow fiber for high harmonic generation.

In Table 1, the maximum photon numbers of the harmonics between the 15th and 25th harmonics from the hollow fiber are summarized, and those from the gas jet reported in a previous work are also listed [5]. The number of focused harmonic photons on target became more than twice as large as that from the pulsed gas jet. We would also like to emphasize that the use of a hollow fiber reduced the load to the exhaust gas system by approximately one-tenth of the use of the gas jet at the maximum output. When the degree of vacuum in the generation chamber was maintained at 1×10^{-3} Torr, the output photon numbers were about seven times more intense than those from the pulsed gas jet. We therefore conclude that the phase matching technique is very useful for improving the conversion efficiency.

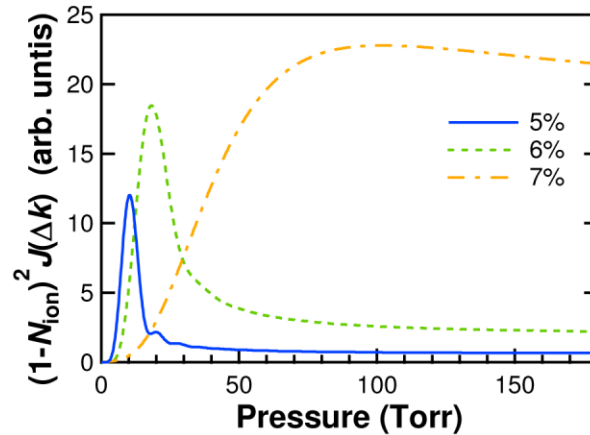


Fig. 4. $(1 - N_{\text{ion}})^2 J(\Delta k)$ as a function of gas pressure, where $J(\Delta k)$ and N_{ion} are the phase mismatch factor and the degree of ionization, respectively. The solid, broken, and dashed-dotted lines correspond to the cases for $N_{\text{ion}} = 0.05, 0.06$, and 0.07 , respectively.

5. Conclusion

In this work, we demonstrated pulse compression of high harmonic pulses from a TDCM and improvement in the conversion efficiency of high harmonic generation achieved through a phase matching technique. The pulse duration of the 21st harmonic was compressed to 11 ± 3 fs by tuning the incident angle in the TDCM, which was equivalent to the appropriate compensation of the pulse-front tilt introduced by diffraction on the grating. The output photons on target were increased by phase matching in a hollow fiber, which made it possible to lengthen the coherence length. The photon fluxes of the 19th harmonic ($= 29.6$ eV) and the 21st harmonic ($= 32.8$ eV) were 7.1×10^9 and 5.7×10^9 photons/s, respectively; these values are comparable to the outputs of synchrotron facilities. Since the separated high harmonic pulses generated by the TDCM have femtosecond pulse durations, it is expected that a high harmonic light source based on a TDCM will provide unique opportunities to gain insight into phenomena inaccessible to synchrotron sources.

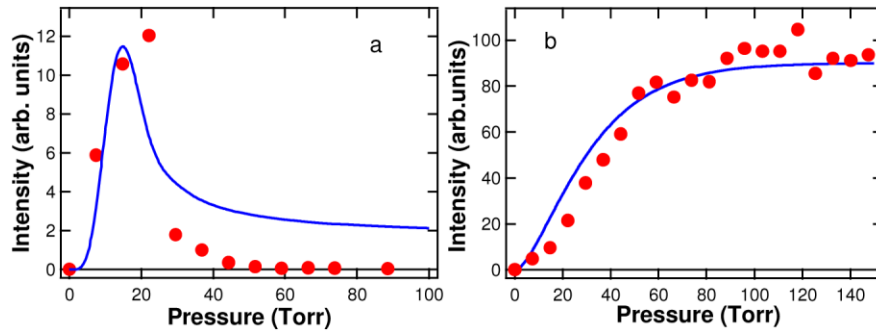


Fig. 5. Pressure dependence of the intensity of the 21st harmonic at a fiber length of (a) 2 cm and (b) 1 cm, represented by solid circles. The solid lines correspond to $(1 - \text{Nion})2J(\Delta k)$. See the text for details.

Table 1. Photon Numbers at the Focus Point of the Time-delay Compensated Monochromator

| Harmonic order | Photon energy (eV) | Photon number per pulse from a hollow fiber ($\times 10^6$) | Photon number per pulse from a pulsed gas jet ($\times 10^6$) ^a |
|----------------|--------------------|---|--|
| 15 | 23.4 | 1.8 | 0.7 |
| 17 | 26.5 | 4.0 | 2.1 |
| 19 | 29.6 | 7.1 | 3.2 |
| 21 | 32.8 | 5.7 | 4.2 |
| 23 | 35.9 | 6.4 | 3.0 |
| 25 | 39.0 | 0.96 | 1.3 |

^a From Ref 5.

Acknowledgments

This work was supported by KAKENHI (23340116 and 23654140), the MATSUO FOUNDATION, the Research Foundation for Opto-Science and Technology, and the “ZE Research Program, IAE, Kyoto University B-8.”